Journal of Zhejiang University-SCIENCE C (Computers & Electronics)
ISSN 1869-1951 (Print); ISSN 1869-196X (Online)
www.zju.edu.cn/jzus; www.springerlink.com
E-mail: jzus@zju.edu.cn

# A differential control method for the proportional directional valve*

Bo JIN[†1], Ya-guang ZHU[1], Wei LI[1], De-sheng ZHANG[1], Lu-lu ZHANG[1], Fei-fei CHEN[2]

([1]*The State Key Laboratory of Fluid Power Transmission and Control, Zhejiang University, Hangzhou 310027, China*)

([2]*Ningbo HOYEA Machinery Manufacture Co., Ltd., Ningbo 315131, China*)

[†]E-mail: bjin@zju.edu.cn

Received Feb. 23, 2014; Revision accepted June 4, 2014; Crosschecked Sept. 17, 2014

**Abstract:** For the proportional directional valve controlled by two proportional solenoids, the normal control method (NCM) energizes only one solenoid at a time. The performance of the valve is greatly influenced by the nonlinearity of the proportional solenoid, such as dead zone and low force gain with a small current, and this effect cannot be eliminated by a simple dead-zone current compensation. To avoid this disadvantage, we propose the differential control method (DCM). By employing DCM, the controller outputs differential signals to simultaneously energize both solenoids of the proportional valve, and the operating point is found by analyzing the force output of the two solenoids to make a minimum variation of the current force gain. The comparisons of the valve response characteristics are made between NCM and DCM by nonlinear dynamic simulation and experiments. Simulation and experimental results show that by using DCM, the frequency response of the valve is greatly enhanced, especially when the input is small, which means that the dynamic characteristics of the proportional valve are improved.

**Key words:** Differential control method, Frequency response, Proportional directional valve, Spool displacement feedback
**doi:**10.1631/jzus.C1400056 **Document code:** A **CLC number:** TP271.3

## 1 Introduction

The electro-hydraulic proportional valves have been widely used in the industry (vehicle, aircraft, mining, etc.) in such applications as contamination prevention and failure maintenance, including some high-precision applications, as their performance is very close to that of electro-hydraulic servo valves, which are much more expensive and consume more energy (Elmer and Gentle, 2001; Liu *et al.*, 2011). Many researchers are active in this field, attempting to improve both the dynamic and static characteristics of the proportional valve.

The performance of the proportional valve is improved by improving hardware of the valve including mechanical structure and electronic devices (Khoshzaban Zavarehi *et al.*, 1999; Li *et al.*, 2001; Del Vescovo and Lippolis, 2003; Amirante *et al.*, 2006) or resorting to recently developed control theories (Sampson *et al.*, 2004). The latter approach is investigated in this paper. Some dynamic performance modeling and simulation studies have recently been presented to predict the dynamic response of proportional solenoid valves, which forms the initial stage of a project aimed at developing an improved controller for the valve (Vaughan and Gamble, 1996; Elmer and Gentle, 2001; Yuan and Li, 2002; Devarajan *et al.*, 2003; Liu *et al.*, 2011; Ruderman and Gadyuchko, 2013). Gamble and Vaughan (1996) presented a comparison between sliding mode control and state feedback and PID control for proportional solenoid valves. The sliding mode controller exhibited the best overall performance in terms of the steady-state error,

* Project supported by the National Natural Science Foundation of China (No. 51221004) and the Program for Zhejiang Leading Team of S&T Innovation (No. 2010R50036)

response time, overshoot, and symmetry. By taking advantage of the solenoid's attraction force characteristic, Kajima (1993) developed a pre-energizing method to energize the solenoid valve, which is highly effective in speeding up the operation of solenoid valves. Amirante *et al.* (2008) used the peak-and-hold technique to achieve an open-loop control of a single stage direct hydraulic proportional valve. This method is characterized by a significantly higher response rate with respect to a standard open-loop control. Amirante *et al.* (2014) proposed an effective methodology for fluid-dynamic design optimization of the sliding spool of a hydraulic proportional directional valve. This method minimizes the flow force at a prescribed flow rate to reduce the required opening force while keeping the operation features unchanged, which allows the operational range of direct driven valves to be enlarged. Kong and Wang (2010) designed a digital state observer feedback control system based on the digital signal processor and the mathematical model of the proportional valve. The accuracy of spool displacement was enhanced and disturbance can be restrained effectively. Bu and Yao (2000) proposed three controllers, including an open-loop compensator based on the pole zero cancellation technique, a full-state feedback adaptive robust controller (ARC), and an output feedback ARC controller, to improve the performance of proportional directional control valves, and showed the advantages and limitations of each method by experiments.

Different from the above-mentioned normal control strategies which energize only one solenoid at a time, we develop a control strategy to energize two solenoids simultaneously by differential signals, which obviously enhances the response of the proportional valve. By adapting this method, the dynamic characteristics of the proportional valve are much improved, as shown by modeling and simulation analysis. Experiments demonstrate the effectiveness of this method.

## 2 Principle of the proportional directional valve and the amplifier card

The hydraulic proportional directional valve (Fig. 1) is a directly controlled component of sub-plate mounting design. The solenoids controlled by the amplifier card operate directly on the slide spool. With both solenoids de-energized, the slide spool is held in the central position by the compression springs. Once one of the proportional solenoids (e.g., solenoid B) is energized, movement of the control spool to the left, which is in proportion to the electrical input signal, will take place. The valve is equipped with a linear variable displacement transducer (LVDT) which converts the motion of the slide spool to a corresponding electrical signal. The signal is sent to the amplifier card as spool position feedback.

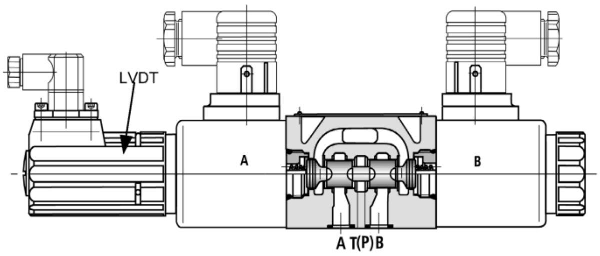


**Fig. 1 Mechanical structure of the proportional valve**

The block diagram of the amplifier card is as shown in Fig. 2. The LVDT is equipped and a controller is proposed for the closed-loop position control. A proportional–integral (PI) controller is adopted for coils current, which can efficiently improve static and dynamic characteristics of the valve. The flutter signal generator, with the purpose of reducing the friction hysteresis loop of the solenoid, makes a great contribution to the performance of the valve in the demanding application. At the current power magnification stage, a pulse width modulation (PWM) current signal is generated with a duty cycle proportional to the input signal, and the current is applied to the solenoid.

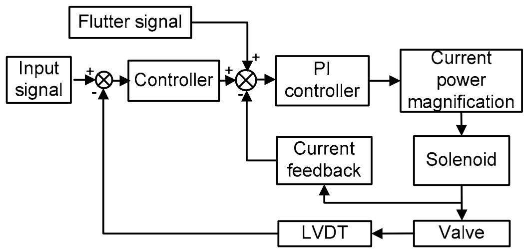


**Fig. 2 Block diagram of the amplifier card**

Since the amplifier card controls the entire sequence and implements closed-loop position control, a general purpose microcontroller with the ARM (Advanced RISC Machines) core is used, which is a powerful tool allowing the designer to create design variations by simply modifying the software. Thus, without adding expensive components, our method can be realized on the above firmware and structure.

## 3 Mathematical model

To present the differential control method, in this section, the mathematical model of the proportional valve is realized, with the characteristics being governed by a couple of solenoid, mechanism, and flow force equations.

### 3.1 Dynamic model of the subsystems

We have investigated different subsystems of the proportional directional valve and derived the governing equations in the form of a differential equation. For simplicity and conciseness of the equation, valve leakage, compressibility of the oil, and the back electromotive coefficient of the coil are neglected.

Solenoid modeling: The solenoid model that consists of an electrical and magnetic circuit has to handle the transformation of the input voltage to an electro-magnetic force on the spool of the valve. The electrical circuit is the actual coil which is represented with a variable inductance $L$ in series with a resistance $R$ of the coil. The voltage acting on the solenoid is corresponding to the control signal. The voltage-current relationship can be derived by (Vaughan and Gamble, 1996)

$$u(t) = L\frac{\mathrm{d}i(t)}{\mathrm{d}t} + i(t)R, \tag{1}$$

where $i(t)$ is the coil current and $u(t)$ is the control voltage.

Although the solenoid used in the valve is termed ‘proportional’, the linear force characteristic can be maintained only for a portion of the full solenoid stroke. Since the solenoid forces are bound up with the coil current and the spool displacement, the relationship between the three variables should be determined for the modeling. The force-current characteristic curves in every 0.0001-m interval of spool displacement have been obtained through the test system for a proportional solenoid (Fig. 3). The data can be described in a table for 2D interpolation. The forces of the solenoid corresponding to the current and the displacement are determined by interpolation within the constructed table. The equation can be defined as

$$F_{\mathrm{m}}(t) = f(i(t), x(t)), \tag{2}$$

where $F_{\mathrm{m}}(t)$ is the electro-magnetic force and $x(t)$ is the displacement of the spool.

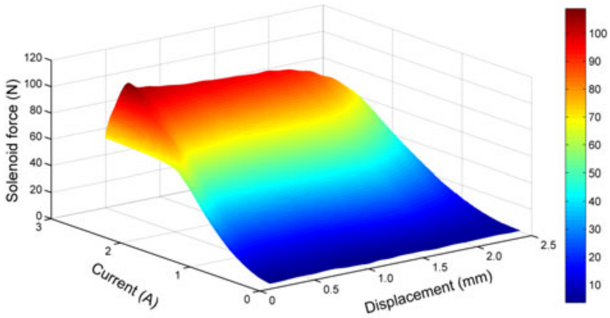


**Fig. 3 Fitted surface of current-displacement-force**

Valve modeling: The valve model consists of a mass of slide spool, compression springs, and a viscous damper under the effect of electro-magnetic and flow forces. It can be represented by Newton’s second law:

$$m\frac{\mathrm{d}^2x(t)}{\mathrm{d}t^2} + B_{\mathrm{v}}\frac{\mathrm{d}x(t)}{\mathrm{d}t} + Kx(t) = F_{\mathrm{m}}(t) - F_{\mathrm{st}} - F_{\mathrm{tr}}, \tag{3}$$

in which $m$ is the spool mass, $B_{\mathrm{v}}$ is the viscous damping coefficient, $K$ is the spring stiffness coefficient, and $F_{\mathrm{st}}$ and $F_{\mathrm{tr}}$ are steady-state and transient flow forces, respectively.

Flow force: Flow induced forces are of two types, steady-state and transient. The formula for the steady-state flow forces is (Yuan and Li, 2002)

$$F_{\mathrm{st}} = \rho Qv\cos\theta, \tag{4}$$

where

$$Q = C_\mathrm{d} A(x)\sqrt{2\Delta P / \rho}, \tag{5}$$

$$v = C_\mathrm{v}\sqrt{2\Delta P / \rho}. \tag{6}$$

From the above equations, the steady-state flow forces are derived:

$$F_\mathrm{st} = 2C_\mathrm{d}C_\mathrm{v}A(x)\Delta P\cos\theta. \tag{7}$$

In the above equations, $\Delta P = P_\mathrm{in} - P_\mathrm{out}$, $P_\mathrm{in}$ and $P_\mathrm{out}$ are inlet and outlet pressures, respectively, $C_\mathrm{d}$ is the discharge coefficient, $C_\mathrm{v}$ is the velocity coefficient, $\rho$ is the density of the hydraulic liquid, $Q$ is the flow rate through the orifice, $v$ is the velocity of the orifice, $\theta$ is the flow angle through the orifice, $x$ is the displacement of the spool, and $A(x)$ is the orifice area corresponding to the opening position.

The transient flow forces are reaction forces on the spool as the fluid in the annular valve chamber accelerates in response to variations in the flow rate. The formula for the transient flow forces is (Yuan and Li, 2002)

$$F_\mathrm{tr} = -\rho l \frac{\mathrm{d}}{\mathrm{d}t}Q = C_\mathrm{d} l\sqrt{2\rho\Delta P}\frac{\mathrm{d}A(x)}{\mathrm{d}t}, \tag{8}$$

where $l$ is the length of the fluid columns for the chamber measured from the port center. Orifice area $A(x)$ is determined by the spool displacement $x$, which will be illustrated later.

Orifice area: The following equations show the cross-section of an orifice with variable round holes:

$$A(x) = \begin{cases} d^2(\theta - \sin\theta)/8, & \alpha < x \le x_\mathrm{max}, \\ 0, & 0 < x \le \alpha, \end{cases} \tag{9}$$

in which

$$\theta = 2\arccos[1 - 2(x-\alpha)/d], \tag{10}$$

$d$ is the hole diameter of the orifice, $\alpha$ is the orifice initial opening, $x$ is the spool displacement from the initial position, and $x_\mathrm{max}$ is the maximum spool displacement.

### 3.2 Dynamic model of the valve

For analysis and simulation, the transfer function of the valve model must be derived. In this study, the friction hysteresis loop of the solenoid is neglected, for the flutter signal of a triangular wave with a tiny amplitude, and a frequency of 220 Hz is used. The nonlinearity of the solenoid forces, however, must be taken into consideration.

For the orifice area, $x$=0.0006 m is selected as the equilibrium point for the Taylor series expansion. $A(x)$ is turned into

$$A(x) = \begin{cases} K_\mathrm{A}x, & \alpha < x \le x_\mathrm{max}, \\ 0, & 0 < x \le \alpha. \end{cases} \tag{11}$$

Thus, the steady-state and transient flow forces can be described as follows:

$$F_\mathrm{st} = 2C_\mathrm{d}C_\mathrm{v}A(x)\Delta P\cos\theta = B_\mathrm{s}x, \tag{12}$$

$$F_\mathrm{tr} = C_\mathrm{d} l\sqrt{2\rho\Delta P}\frac{\mathrm{d}A(x)}{\mathrm{d}t} = B_\mathrm{t}\frac{\mathrm{d}x}{\mathrm{d}t}, \tag{13}$$

where $B_\mathrm{s}$ is the stiffness of the steady-state flow forces and $B_\mathrm{t}$ is the damping coefficient of the transient flow forces.

By Laplacian transformation of Eqs. (1)–(3), (11)–(13), the transfer functions are derived:

Coil current transfer function:

$$I(s) = \frac{U(s)}{Ls + R}. \tag{14}$$

Electro-magnetic transfer function:

$$F_\mathrm{m}(s) = F(I(s), X(s)). \tag{15}$$

The force executed on the spool:

$$F_\mathrm{m}(s) = F_{\mathrm{m}A}(s) - F_{\mathrm{m}B}(s). \tag{16}$$

Valve transfer function:

$$X(s) = \frac{F_\mathrm{m}(s)}{ms^2 + (B_\mathrm{v} + B_\mathrm{t})s + (K + B_\mathrm{s})}. \tag{17}$$

The block diagram of the valve system is shown in Fig. 4.

### 3.3 Presentation and analysis of DCM

As shown in Fig. 4, the force exerted on the spool is the composition of the solenoid forces, which

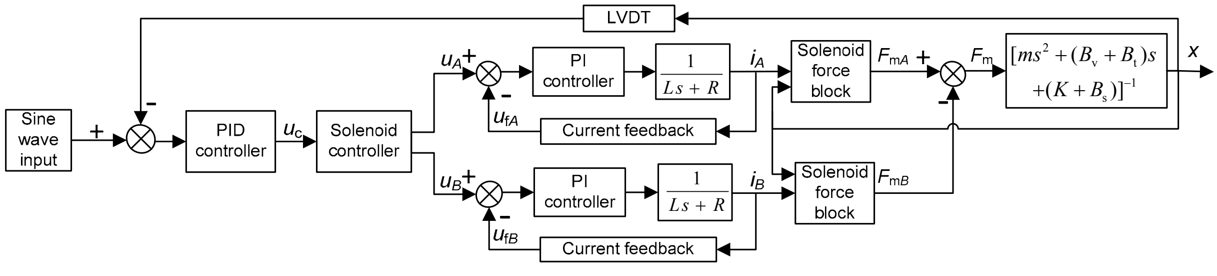


**Fig. 4 Block diagram of the valve system**

can be derived in the form of

$$F_{\mathrm{m}}(i(t),x(t))=F_{\mathrm{m}A}(i_A(t),x(t))-F_{\mathrm{m}B}(i_B(t),x(t)),\quad(18)$$

where $F_{\mathrm{m}A}(t)$ and $F_{\mathrm{m}B}(t)$ are the forces of solenoids $A$ and $B$, respectively, $F_{\mathrm{m}}(t)$ is the composite force of the solenoid exerted on the spool, and $i_A(t)$ and $i_B(t)$ are the control instructions outputted to solenoids $A$ and $B$, respectively.

The composite force is the main factor affecting the performance of the valve. It is quite different in the normal control method and our proposed control strategy. The normal control method (NCM) of the valve needs to be described first.

With NCM, in proportion to each signal input, a certain balance point between the spring and the force of one solenoid determines a particular spool stroke and spool position. The input signal of the valve could be either positive or negative. However, only one of the solenoids is working at a time. That is to say, if one solenoid is energizing, the other solenoid will be in the de-energized state. The solenoid controller in Fig. 4 can be represented as

$$\begin{cases}u_A(t)=u_{\mathrm{c}}(t),\ \ u_B(t)=0, & \text{if } u_{\mathrm{c}}(t)>0,\\ u_A(t)=0,\ \ u_B(t)=u_{\mathrm{c}}(t), & \text{if } u_{\mathrm{c}}(t)<0,\end{cases}\quad(19)$$

where $u_A(t)$ and $u_B(t)$ are the control instructions of solenoids $A$ and $B$, respectively, and $u_{\mathrm{c}}(t)$ is the control instruction converted from the displacement controller.

Since the current control signal is in proportion to the control signal $u(t)$, we have

$$i_{\mathrm{c}}(t)=k_{\mathrm{c}}u_{\mathrm{c}}(t),\quad(20)$$

in which $k_{\mathrm{c}}$ is the proportionality coefficient between $i_{\mathrm{c}}(t)$ and $u_{\mathrm{c}}(t)$.

Thus, Eq. (19) can be formulated in current form:

$$\begin{cases}i_A(t)=i_{\mathrm{c}}(t),\ \ i_B(t)=0, & \text{if } i_{\mathrm{c}}(t)>0,\\ i_A(t)=0,\ \ i_B(t)=i_{\mathrm{c}}(t), & \text{if } i_{\mathrm{c}}(t)<0.\end{cases}\quad(21)$$

Eq. (18) can be transformed to

$$F_{\mathrm{m}}(i(t),x(t))=\begin{cases}F_{\mathrm{m}A}(i_{\mathrm{c}}(t),x(t)), & i_{\mathrm{c}}(t)>0,\\ -F_{\mathrm{m}B}(i_{\mathrm{c}}(t),x(t)), & i_{\mathrm{c}}(t)<0.\end{cases}\quad(22)$$

By this kind of control strategy, the force exerted on the spool is supplied by only one of the solenoids. The total force output of the two solenoids is shown in Fig. 5. The current force gain is very small and has a rather large change within the whole working space. Thus, in the whole solenoid stroke, nonlinear characteristics obviously and directly affect the dynamic performance of the valve. If the current operating point is over 500 mA, the current force gain would stay between 0.028 and 0.052 N/mA.

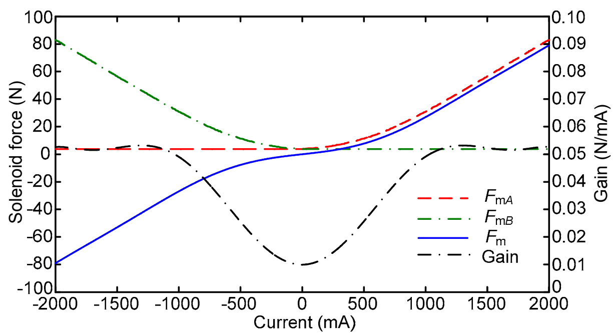


**Fig. 5 Current-force characteristic and current-gain curve of solenoid**

To solve this problem, DCM is proposed to avoid the disadvantages induced by the alternate energizing and small current force gain. A basic signal is applied to both solenoids and the control signal $u_c(t)$ works differentially on each solenoid; hence, both solenoids work in their linear regions. The solenoid controller in Fig. 4 can be defined as

$$u_A(t) = u_0 + u_c(t), \quad u_B(t) = u_0 - u_c(t). \tag{23}$$

It can also be formulated in current form:

$$i_A(t) = i_0 + i_c(t), \quad i_B(t) = i_0 - i_c(t). \tag{24}$$

$u_0$ and $i_0$ are the quiescent operating points.

Consequently, both solenoids are energized if the valve is in an active state. The composition of solenoid forces is

$$F_m(i,x) = F_{mA}(i_0 + i_c(t), x(t)) - F_{mB}(i_0 - i_c(t), x(t)). \tag{25}$$

In this way, the composition of the solenoid forces is related to the current control signal and the displacement of the spool. Thus, the current-force characteristic for a certain $i_0$ and $x$ can be obtained. As shown in Fig. 6, at any displacement of the spool, characteristics of the composition force are determined by the characteristic of the solenoids and the quiescent operating point $i_0$. That is to say, a good selection of the quiescent operating point makes a good characteristic.

The current force gain is

$$g(i) = \frac{\partial F_{Dm}(i,x)}{\partial i}, \tag{26}$$

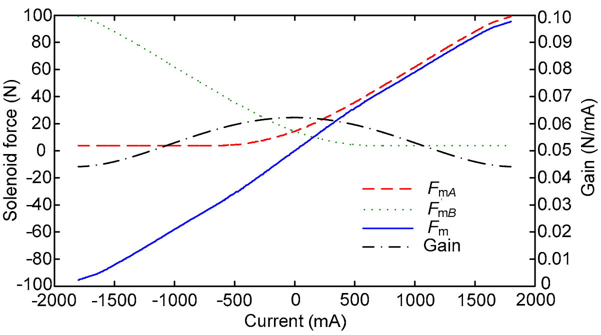


**Fig. 6 Current-force characteristic and current-gain curve of the composite force at $i_0$=600 mA, $x$=0.001 mm**

and the variation of the gain is

$$\xi = \frac{\max(g(i)) - \min(g(i))}{\max(g(i))}. \tag{27}$$

When the quiescent operating point $i_0$ is changed, the gain curve of current force will be changed, so does $\xi$. The results are shown in Fig. 7. The minimum variation of the current force gain standing for better linearity characteristics of the composite force is achieved at $i_0$=500 mA. Additionally, in view of the single solenoid characteristic, at $i_0$=500 mA the drawbacks of the dead zone can be overcome. Thus, the result should be acceptable and can be used in the following simulations and experiments.

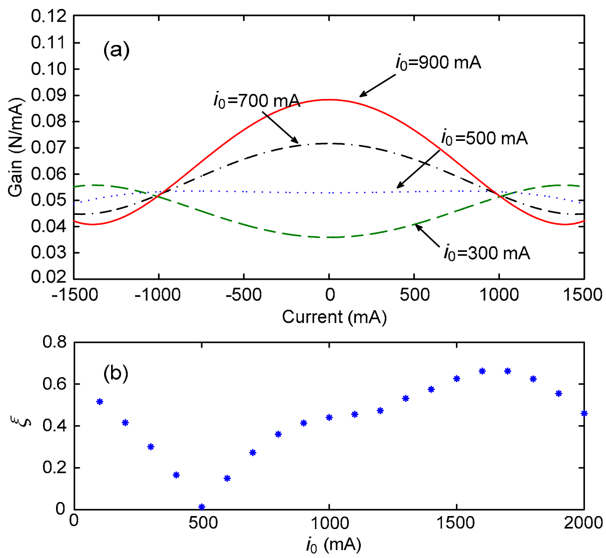


**Fig. 7 Variations of the current force gain at different currents: (a) current force gain; (b) variation of current force gain**

## 4 Simulation and analysis

To verify the effectiveness of DCM, a simulation model was established according to the transfer functions of the valve system in Eqs. (14)–(17). Since the control algorithm is not the main point of this study, the classical proportional–integral–derivative (PID) controller and PI controller were used. The PID controller was employed for closed-loop control of the spool position. Simultaneously, the PI controller was used to control the coil current. In view of the requirements for stability and good transient performance, the orthogonal experimental method (Jin *et al.*, 2013) was used for PID parameter tuning. The main parameters of the simulation are shown in Table 1.

**Table 1 Parameters of the system**

| Parameter | Value | Parameter | Value |
|---|---|---|---|
| $L$ | 0.01 H | $\rho$ | 850 kg/m$^3$ |
| $R$ | 2.7 Ω | $l$ | 0.012 m |
| $m$ | 0.064 kg | $u_0$ | 2 V |
| $B_v$ | 80 N·s/m | $i_0$ | 0.5 A |
| $K$ | 21 000 N/m | $K_A$ | 0.00212 m |
| $C_d$ | 0.61 | $B_s$ | 3643.7 N/m |
| $C_v$ | 0.98 | $B_t$ | 2.57 N·s/m |
| $\theta$ | 69 deg | $\alpha$ | 0.0004 m |
| $d$ | 0.007 m | | |

The simulation model was developed based on the diagram shown in Fig. 4. In NCM, a current compensation, which can be figured out by Eq. (28), is usually supplied by a step generator to skip the dead zone where the force gain of the solenoid is quite small with a small current, as shown in Fig. 5. The solenoid controller is defined by Eq. (19). In DCM, however, the solenoid controller is a differential controller defined by Eq. (23) to energize both solenoids. The compensation can be removed.

$$U_{step}=\mathrm{sgn}(U_c)U_{min}, \tag{28}$$

where $U_{min}$ is the minimum control voltage to skip the dead zone, and $U_{step}$ is the compensation signal.

The current in the coil and the displacement of the spool are the main factors that influence the electro-magnetic force. In the simulation model, the calculation of the solenoid forces through the interpolation method is included in the solenoid force block as shown in Fig. 3.

Fig. 8 shows the currents of the coil under different methods at 50%/20 Hz sine wave input. DCM made the valve serve around the quiescent operating point, which was completely in the linear region. The influence of nonlinear characteristics was almost eliminated and the response of the valve consequently enhanced. With NCM, however, the solenoids sometimes worked with small currents (less than 200 mA), and the solenoids outputted very small force. Hence, the valve works more slowly.

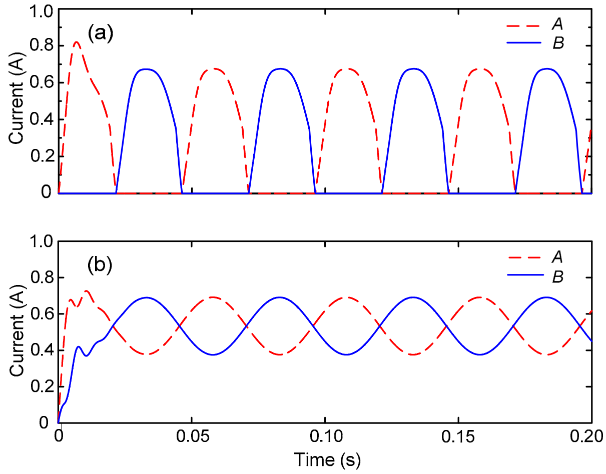


**Fig. 8 Coil currents: (a) NCM; (b) DCM**

This effect is shown in Fig. 9. When the input was a sine wave at 1 Hz with 50% maximum amplitude, the waveform distortion was diminished using the compensation and eliminated by DCM. Generally, the waveform distortion of spool displacement as shown in Fig. 9a is caused by the current dead zone of the solenoid. A small compensation value is almost invalid for the distortion, while a large value will cause instability in the valve. This is why the waveform distortion cannot be eliminated completely by step compensation (Fig. 9b). Differently, the DCM method which serves out of the dead zone can actuate the spool quickly without waveform distortion (Fig. 9c).

In Fig. 10, by changing the amplitude and frequency of the sine wave input, the frequency responses of the spool displacement at different inputs can be obtained. Obviously, the dynamic characteristics of the system under DCM are better than those under NCM.

## 5 Test rig and experiment validation

To validate the proposed control method, experiments were carried out on the test rig (Fig. 11). The system included an internal gear pump (IGT-1-10, working pressure 31.5 MPa) driven by an electric motor, providing an output flow rate of 160 L/min. Two relief valves (maximum working pressure 35 MPa)

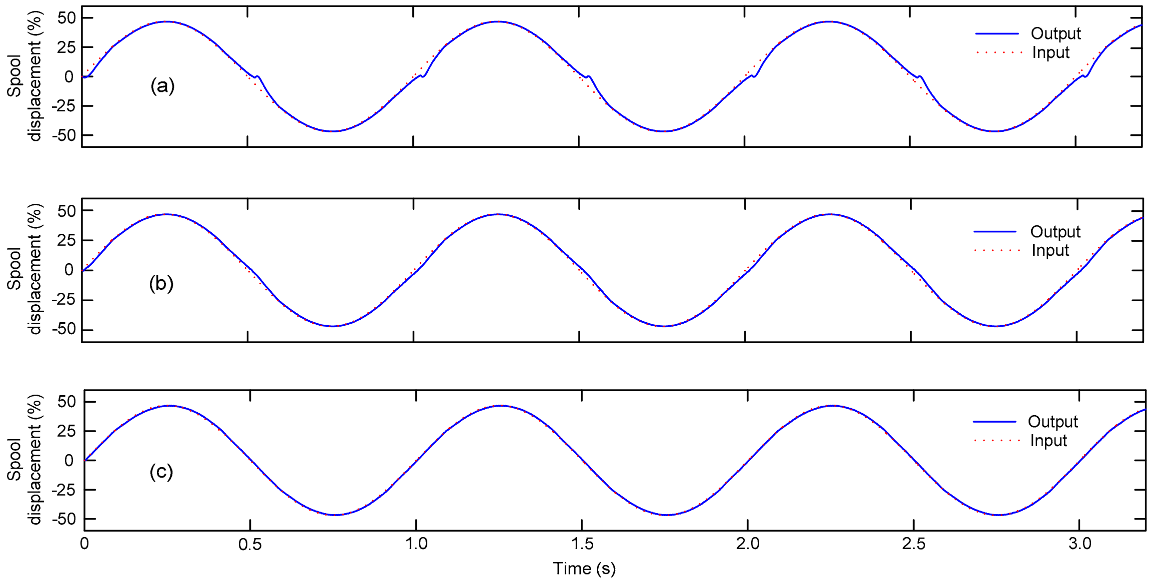


**Fig. 9  Responses of 50%/1 Hz sine wave input: (a) NCM without compensation; (b) NCM with compensation; (c) DCM**

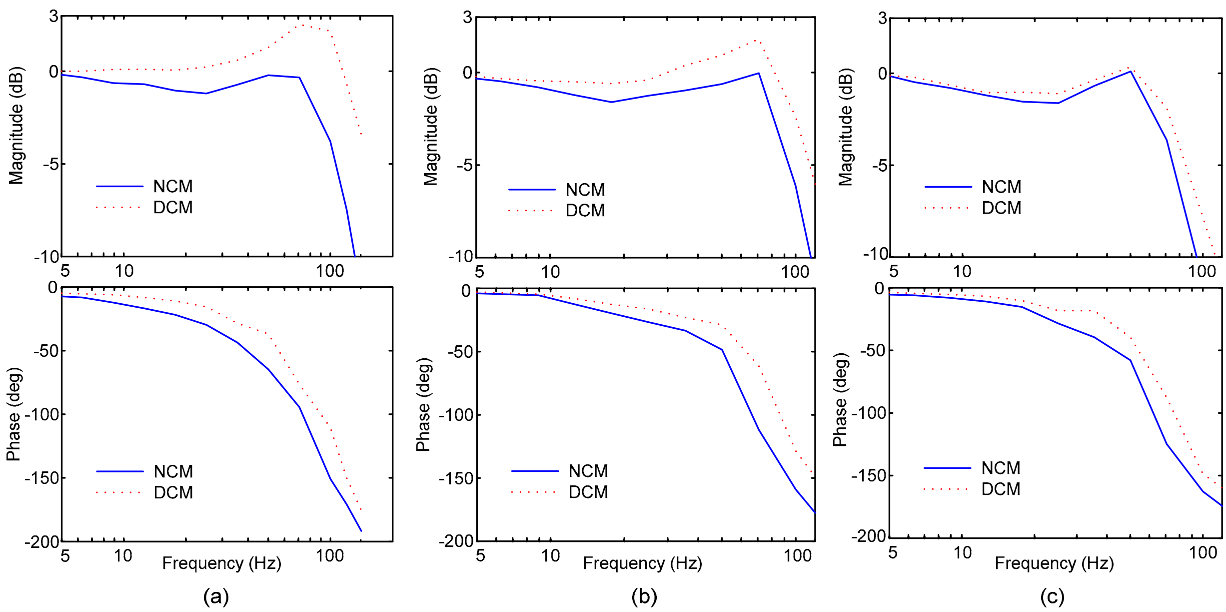


**Fig. 10  Bode diagrams at different inputs: (a) 25%; (b) 50%; (c) 100%**

were used: one was to set up the system pressure, and the other to set up the pressure of the oil return. A manual valve (working pressure 31.5 MPa) was used as the main switch of the rig, and two one-way throttle valves (maximum working pressure 35 MPa) were used to apply load pressure. In the apparatus, the control signal, which was supplied by a low frequency signal generator (LFSG), was used to control the proportional direction valve through the amplifier card. The LVDT (frequency>100 Hz, output DC ±5 V) was equipped to convert the spool displacement signal to the voltage, which was actually sent to the data acquisition unit (5 kHz, 12-bit resolution) of the amplifier card. The input signal and displacement signal were displayed and stored by the oscilloscope. The picture of the test rig is shown in Fig. 12.

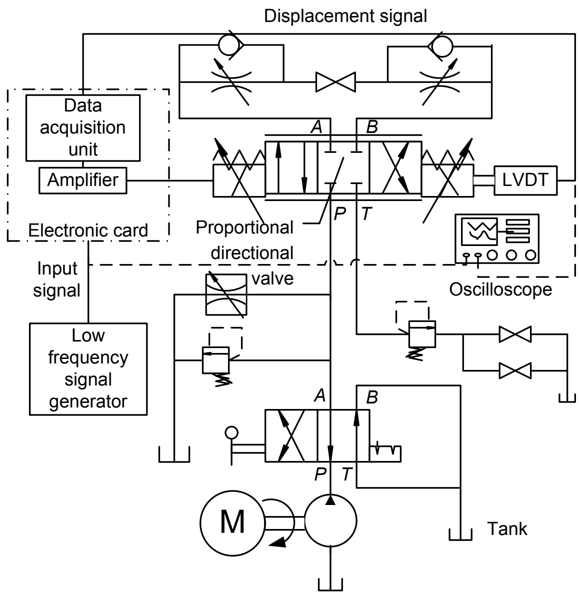


**Fig. 11 Schematic diagram of the experiment system**

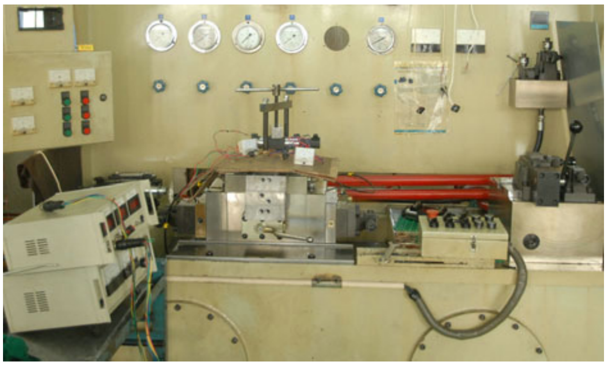

**Fig. 12 Photograph of the test rig**

In the experiment, the pressure differences between the valve inlet and outlet were adjusted to 1 MPa by the relief valves. The responses of different step inputs are shown in Fig. 13. Since PID parameters were tuned with 50% input, both methods performed well. Obviously, the rise time of NCM was almost identical to that of DCM, but the settling time of the normal method was much longer. That is to say, DCM has a better performance at different inputs.

Fig. 14 gives the responses of 50%/1 Hz sine wave input to illustrate the effect of DCM on the dynamic characteristics of the valve. The responses were the same as the simulation results. A large control error occurred near the zero spool position with NCM without compensation (Fig. 14a). This error was greatly reduced by compensation (Fig. 14b), and eliminated with DCM (Fig. 14c). Note that the waveform distortion in the experiments was much larger than that in the simulations because of the friction, and the effect of compensation in NCM was limited, but DCM still performed well.

By changing the amplitude and frequency of the sine wave input of LFSG, the frequency responses of spool displacement can be obtained (Fig. 15). The amplitude attenuation under DCM was much lower than that of the normal method at 25% and 50% input. This is because the nonlinear characteristic is manifest when the solenoid current is small; when DCM is employed, the influence of the nonlinear characteristic is almost eliminated.

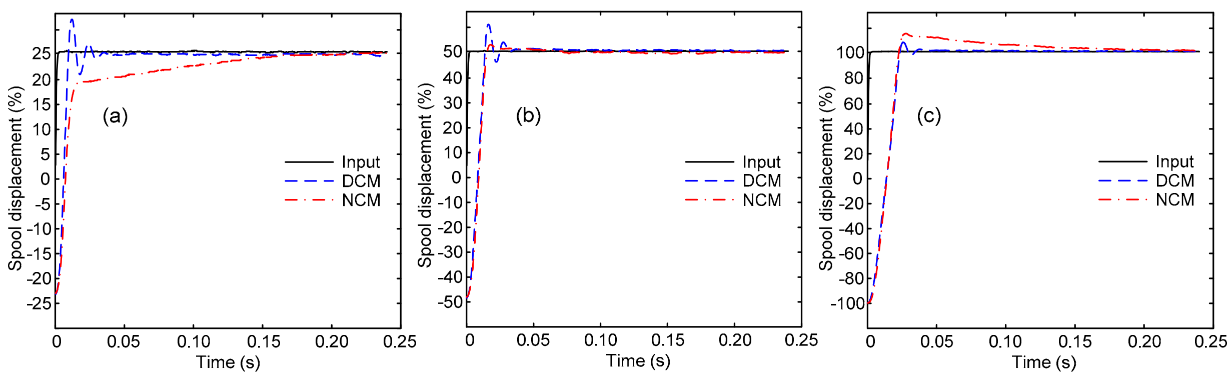


**Fig. 13 Responses of different step inputs: (a) 25%; (b) 50%; (c) 100%**

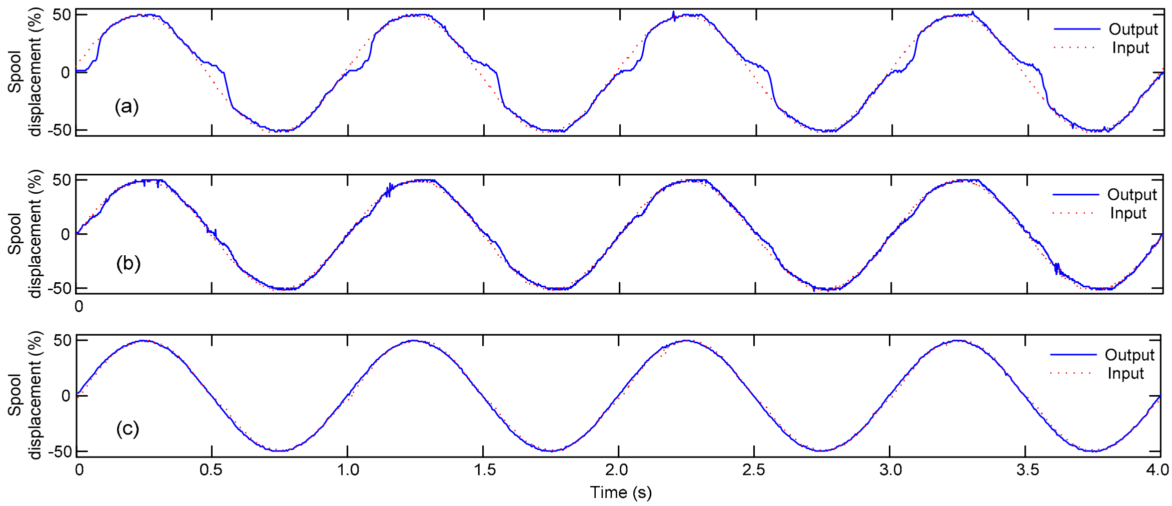


**Fig. 14 Responses of 50%/1 Hz sine wave input: (a) NCM without compensation; (b) NCM with compensation; (c) DCM**

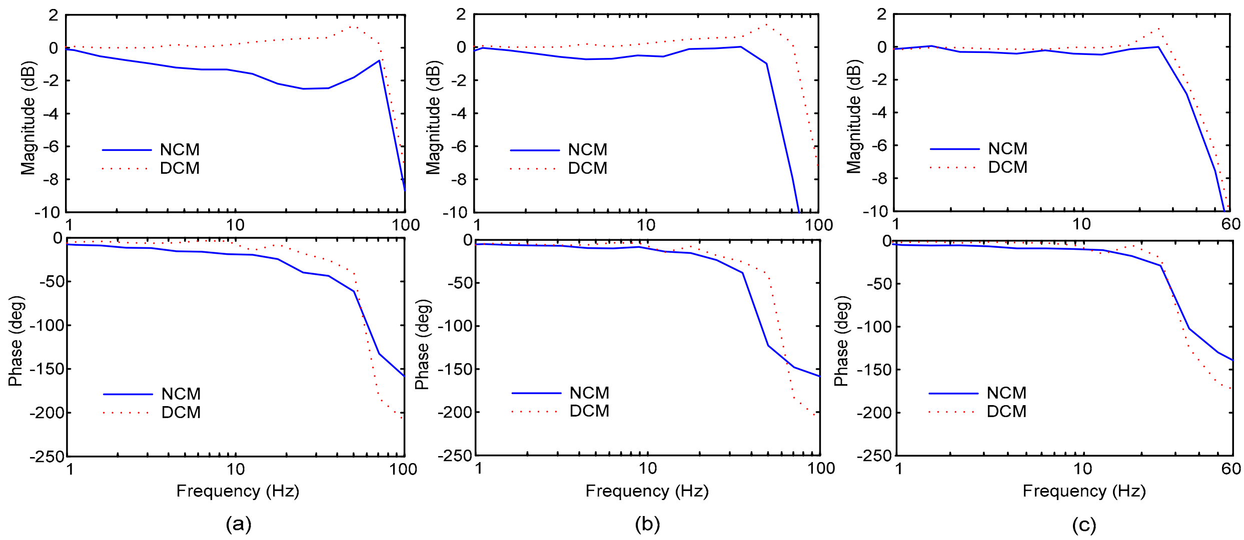


**Fig. 15 Bode diagrams of experiments at different inputs: (a) 25%; (b) 50%; (c) 100%**

## 6 Conclusions

This paper primarily presents a new control strategy named the differential control method for the proportional directional valve with spool position feedback to improve its dynamic and static characteristics. Comparisons were made between DCM and NCM in a nonlinear model. According to simulation results, the proposed method was analyzed to explain why it is better than the normal ones, and the quiescent operating point of DCM was shown to make a minimum variation in the current force gain. Experiments were conducted to prove that our method is practical and effective.

Using the proposed method, the frequency response of the valve can be enhanced, and the waveform distortion greatly reduced. Therefore, the proportional valve can be used in applications with higher frequency responses and higher precision requirements. Based on the experiment results, the waveform distortion is apparently reduced using our method, as the solenoids completely operate in the linear region. Also, the implementation cost of the proposed method is very low, mainly because the control theory is concise and straightforward to implement in software. The process of the method indicates that some advanced control theories and methods can be combined, which means further improvement could be achieved without much effort.

## References

Amirante, R., Del Vescovo, G., Lippolis, A., 2006. Flow forces analysis of an open center hydraulic directional control valve sliding spool. *Energ. Conv. Manag.*, **47**(1): 114-131. [doi:10.1016/j.enconman.2005.03.010]

Amirante, R., Innone, A., Catalano, L.A., 2008. Boosted PWM open loop control of hydraulic proportional valves. *Energ. Conv. Manag.*, **49**(8):2225-2236. [doi:10.1016/j.enconman.2008.02.001]

Amirante, R., Catalano, L.A., Poloni, C., *et al.*, 2014. Fluid-dynamic design optimization of hydraulic proportional directional valves. *Eng. Optim.*, **46**(10):1295-1314. [doi:10.1080/0305215X.2013.836638]

Bu, F., Yao, B., 2000. Performance improvement of proportional directional control valves: methods and experiments. Proc. ASME Dynamic Systems and Control Division, p.297-304.

Del Vescovo, G., Lippolis, A., 2003. Three-dimensional analysis of flow forces on directional control valves. *Int. J. Fluid Power*, **4**(2):15-24. [doi:10.1080/14399776.2003.10781162]

Devarajan, D., Stanton, S., Knorr, B., 2003. Multi-domain modeling and simulation of a linear actuation system. Proc. Int. Workshop on Behavioral Modeling and Simulation, p.76-81. [doi:10.1109/BMAS.2003.1249861]

Elmer, K.F., Gentle, C.R., 2001. A parsimonious model for the proportional control valve. *Proc. Inst. Mech. Eng. C J. Mech. Eng. Sci.*, **215**(11):1357-1363. [doi:10.1243/0954406011524739]

Gamble, J.B., Vaughan, N.D., 1996. Comparison of sliding mode control with state feedback and PID control applied to a proportional solenoid valve. *J. Dynam. Syst. Meas. Contr.*, **118**(3):434-438. [doi:10.1115/1.2801163]

Jin, B., Zhu, Y.G., Li, W., 2013. PID parameters tuning of proportional directional valve based on multiple orthogonal experiments method: method and experiments. *Appl. Mech. Mater.*, **325**:1166-1169. [doi:10.4028/www.scientific.net/AMM.325-326.1166]

Kajima, T., 1993. Development of a high-speed solenoid valve-investigation of the energizing circuits. *IEEE. Trans. Ind. Electron.*, **40**(4):428-435. [doi:10.1109/41.232232]

Khoshzaban Zavarehi, M., Lawrence, P.D., Sassani, F., 1999. Nonlinear modeling and validation of solenoid-controlled pilot-operated servovalves. *IEEE/ASME Trans. Mechatron.*, **4**(3):324-334. [doi:10.1109/3516.789690]

Kong, X., Wang, H., 2010. A spool displacement control system of proportional valve based on digital observer. *Key Eng. Mater.*, **455**:110-115. [doi:10.4028/www.scientific.net/KEM.455.110]

Li, K., Mannan, M.A., Xu, M., *et al.*, 2001. Electro-hydraulic proportional control of twin-cylinder hydraulic elevators. *Contr. Eng. Pract.*, **9**(4):367-373. [doi:10.1016/S0967-0661(01)00003-X]

Liu, Y., Dai, Z., Xu, X., *et al.*, 2011. Multi-domain modeling and simulation of proportional solenoid valve. *J. Cent. South Univ. Technol.*, **18**(5):1589-1594. [doi:10.1007/s11771-011-0876-2]

Ruderman, M., Gadyuchko, A., 2013. Phenomenological modeling and measurement of proportional solenoid with stroke-dependent magnetic hysteresis characteristics. IEEE Int. Conf. on Mechatronics, p.180-185. [doi:10.1109/ICMECH.2013.6518532]

Sampson, E., Habibi, S., Burton, R., *et al.*, 2004. Effect of controller in reducing steady-state error due to flow and force disturbances in the electrohydraulic actuator system. *Int. J. Fluid Power*, **5**(2):57-66. [doi:10.1080/14399776.2004.10781192]

Vaughan, N.D., Gamble, J.B., 1996. The modeling and simulation of a proportional solenoid valve. *J. Dynam. Syst. Meas. Contr.*, **118**(1):120-125. [doi:10.1115/1.2801131]

Yuan, Q., Li, P.Y., 2002. An experimental study on the use of unstable electrohydraulic valves for control. American Control Conf., p.4843-4848. [doi:10.1109/ACC.2002.1025425]